Isotopes, Ice Ages, and Terminal Proterozoic Earth History

Proc. Natl. Acad. Sci. USA
Vol. 94, pp. 6600–6605, June 1997
Geology

Isotopes, ice ages, and terminal Proterozoic earth history

(carbon isotopes/stratigraphy/paleontology/Ediacaran fauna)

ALAN J. KAUFMAN*, ANDREW H. KNOLL*†, AND GUY M. NARBONNE‡

*Botanical Museum, Harvard University, Cambridge, MA 02138; and ‡Department of Geological Sciences, Queens University, Kingston, Ontario, K7L 3N6 Canada

Contributed by Andrew H. Knoll, April 18, 1997

ABSTRACT **Detailed correlations of ancient glacial deposits, based on temporal records of carbon and strontium isotopes in seawater, indicate four (and perhaps five) discrete ice ages in the terminal Proterozoic Eon. The close and repeated stratigraphic relationship between C-isotopic excursions and glaciogenic rocks suggests that unusually high rates of organic carbon burial facilitated glaciation by reducing atmospheric greenhouse capacity. The emerging framework of time and environmental change contributes to the improved resolution of stratigraphic and evolutionary pattern in the early fossil record of animals.**

In 1964, W. B. Harland (1) proposed that an ice age of global extent occurred near the end of the Proterozoic Eon. He recognized a worldwide distribution of tillites and associated lithologies beneath strata bearing Ediacaran fossils and considered that these rocks were deposited during surface refrigeration more pronounced than the Pleistocene ice age. Debate engendered by Harland's hypothesis continues to the present. Are geographically scattered tillites demonstrably synchronous? How many ice ages occurred, if indeed they compose discrete events? And, does late Cenozoic climatic change provide an appropriate model for more ancient glaciations?

The demonstration that the carbon and strontium isotopic composition of seawater varied systematically through the Neoproterozoic Era [1000–543 million years ago (Ma); refs. 2, 3] provides a stratigraphic framework with the potential to resolve fundamental questions of tillite correlation. At the same time, chemostratigraphic data may constrain hypotheses to explain Neoproterozoic climatic oscillations. The C-isotopic record through this interval is characterized by unusual ^{13}C enrichment in carbonates and organic matter, punctuated by excursions to unusually low $\delta^{13}C$ values. Some, and perhaps all, of these strong negative excursions are associated with glaciogenic rocks (4, 5). If general, this suggests that Neoproterozoic climatic change was mediated, at least in part, by oceanographically driven variations in carbon cycling. Here we present new data from Neoproterozoic successions in northwestern Canada and Spitsbergen, focusing on glacial intervals not previously sampled, and we use integrated stratigraphic techniques to predict worldwide correlations of ancient tillites. The resulting chronostratigraphic framework provides an improved perspective on the relationship between terminal Proterozoic environmental change and early animal evolution.

Chemostratigraphy of Tillite-Bearing Successions: Northwestern Canada

Late Neoproterozoic strata in the Mackenzie Mountains (Fig. 1) compose the Windermere Supergroup, a 5-km thick succession that records the breakup of a supercontinent and the opening of the proto-Pacific Ocean (6). Most units are of deep water origin and lack strong evidence of secondary alteration. Glaciogenic deposits occur at two distinct stratigraphic levels in the Windermere succession. The first is represented by the Rapitan Group, a succession of mudstones, rhythmites, iron formation, and glacial diamictites (7, 8) that has been correlated on lithostratigraphic grounds with Sturtian (*ca.* 750–700 Ma) tillites in Australia (8). Evidence of a second Windermere ice age is preserved in the Ice Brook Formation (9, 10). Ice Brook tillites are thought to be correlative with those of the Elatina Formation in South Australia (7–10) and Varanger (*ca.* 570–610 Ma; ref. 11) glaciogenic rocks in the North Atlantic region.

A maximum age for the Windermere succession is provided by U-Pb zircon dates of 778–779 Ma for igneous intrusions in underlying formations (12, 13). A U-Pb zircon age date on a granite clast within the Rapitan tillite indicates that this ice age is no older than 755 ± 18 Ma (14). Windermere rocks contain an outstanding record of early animal fossils, with three distinct assemblages of Ediacara-type remains occurring through more than 2.5 km of strata (15, 16). The lowermost assemblage (I) occurs below the Ice Brook tillite. It contains simple discs and rings that may represent the oldest animals yet discovered (17). More diverse and structurally complex remains occur above the tillite in the Sheepbed Formation. Simple, radially symmetrical fossils, including the widespread Ediacaran genus *Cyclomedusa* (assemblage IIA), first appear near the middle of the formation; a more diverse assemblage (IIB), which includes the simple forms encountered lower in the section, more complex discs, and rare fronds (18), occurs throughout the upper third of the unit. The most diverse Ediacaran assemblage (III) occurs in the overlying Blueflower Formation; fossils found here include those known from assemblage II, along with a greater variety of discs, fronds, and, for the first time, dickinsoniids and abundant trace fossils. These fossils are thought to be coeval with the Schwarzrand assemblage in Namibia, the Ediacara assemblage in the Pound Quartzite of Australia, and several other localities worldwide (16).

The results of C- and Sr-isotopic analyses of Windermere samples are shown in Fig. 1; new collections from the Twitya, Keele, and lower Sheepbed formations augment analyses reported earlier (16). All samples were subjected to a battery of petrographic, elemental, and isotopic tests to establish whether they preserve little-altered C-isotopic compositions, but the most persuasive evidence that stratigraphic variations reflect temporal changes in seawater chemistry is the covariation of $\delta^{13}C$ in microspar carbonate and coexisting organic C. The nearly identical isotopic trends seen in upper Windermere carbonates and organic C are offset by a relatively constant value (*ca.* 28‰) only slightly larger than the difference between primary carbonates and organic matter in modern oceans (19–21). No known diagenetic or metamorphic pro-

The publication costs of this article were defrayed in part by page charge payment. This article must therefore be hereby marked "*advertisement*" in accordance with 18 U.S.C. §1734 solely to indicate this fact.

†To whom reprint requests should be addressed. e-mail: aknoll@oeb.harvard.edu.

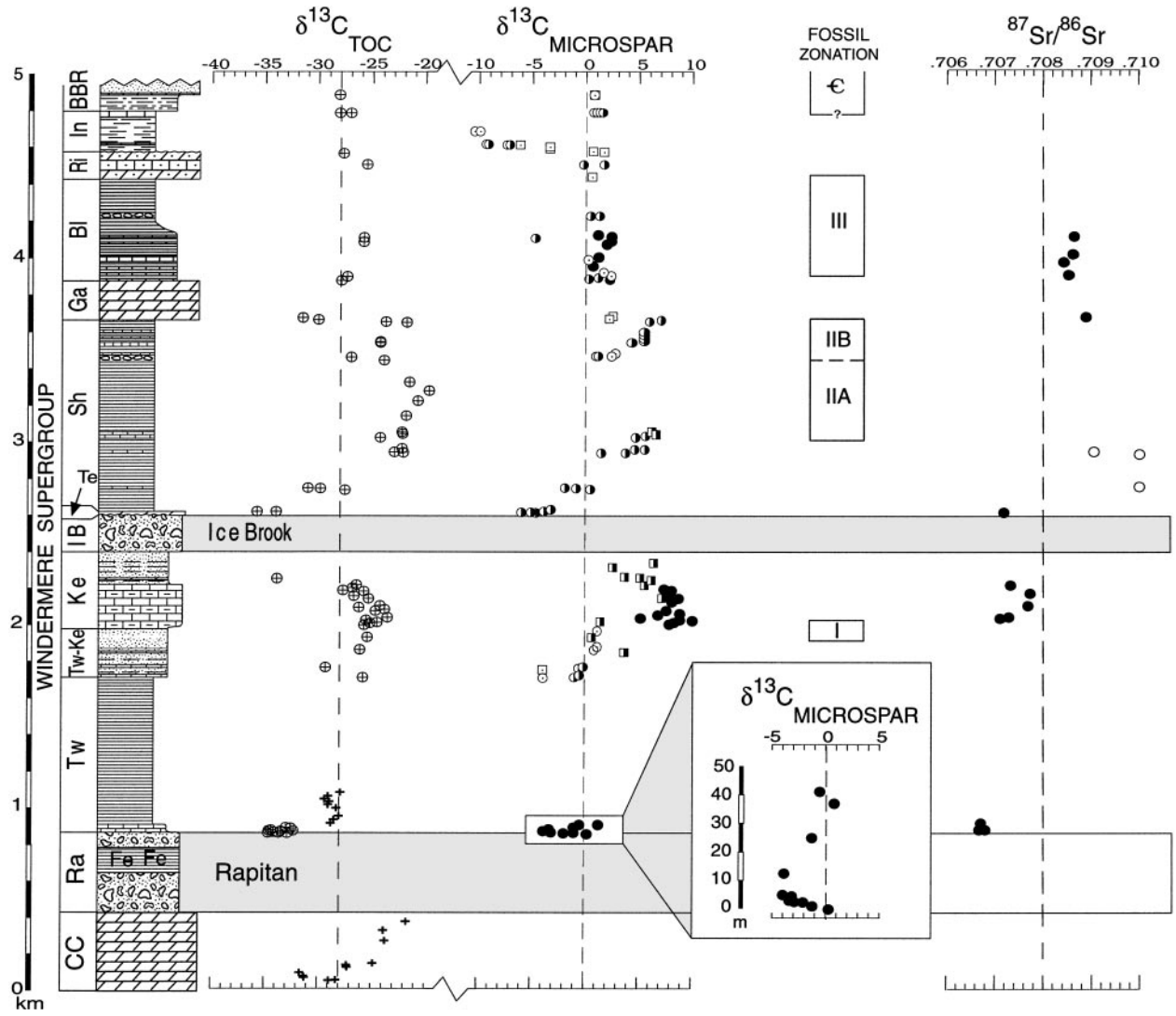

FIG. 1. Temporal variations in $\delta^{13}C$ of carbonates and coexisting organic matter, Ediacaran and Early Cambrian fossil zonation, and $^{87}Sr/^{86}Sr$ changes recorded in limestones through the upper Windermere Supergroup, northwest Canada. Lithologic evidence of glaciation is preserved in the Ice Brook and Rapitan tillites. Organic C analyses of Coppercap and lower Twitya formation samples (+) are from Strauss and Moore (22). Other carbonate symbols indicate the degree of secondary alteration determined through petrographic, elemental, and isotopic analyses (cf. ref. 16); filled symbols represent least-altered samples. A composite $\delta^{13}C$ curve that integrates carbonate and organic carbon data is shown in Fig. 4*C*. Fossil zonation: I, small, simple discs; IIA, larger, radially symmetrical discs; IIB, complex discs and fronds; III, complex discs, fronds, dickinsoniids, and abundant trace fossils; C, small shelly fossils of Early Cambrian aspect. Stratigraphic abbreviations: Fm., formation; BBR, Backbone Ranges Fm.; In, Ingta Fm.; Ri, Risky Fm.; Bl, Blueflower Fm.; Ga, Gametrail Fm.; Sh, Sheepbed Fm.; Te, Tepee Fm.; IB, Ice Brook Fm.; Ke, Keele Fm.; Tw-Ke, Twitya–Keele transitional interval; Tw, Twitya Fm.; Ra, Rapitan Group; CC, Copper Cap Fm.

cesses alter both carbon reservoirs in the same direction to the same extent (4).

The Windermere C-isotopic record is characterized by repeated strong positive-to-negative $\delta^{13}C$ excursions (Fig. 1). They occur at the base of the Twitya Formation in ribbon limestones that cap Rapitan tillites, in uppermost Keele to basal Sheepbed units associated with the Ice Brook tillite, and within the middle Sheepbed Formation. In basal Twitya limestones immediately above the Rapitan tillite, $\delta^{13}C$ values shift rapidly from near 0 to $-5‰$ in the first 10 m of section and then return to values as high as $+1.5‰$ over the next 30 m (see *Inset* in Fig. 1). Carbonates in the Coppercap Formation immediately beneath Rapitan tillites have not yet been measured, but analyses of organic matter (22) indicate significant enrichment in ^{13}C near the top of the unit. Higher in the Windermere succession, C-isotopic data for the Keele Formation display an impressive richness of information. The Twitya–Keele transition shows values near $0‰$, above which there is a marked excursion to $+10‰$. There is second order structure evident within this excursion, above which C-isotopic values remain positive ($+3‰$) to the top of the main Keele carbonate sequence. Depositional $\delta^{13}C$ values of the magnitude recorded in the Keele peak are known for only one other time in Earth history, an interval *ca.* 2100 Ma ago when the oxidation state of the biosphere is thought to have increased (23–27). For this reason, the Keele peak should provide a reliable stratigraphic marker that can be identified in widely distributed carbonate successions; it also marks the position of the simple discs and rings of the oldest known Ediacara-type biota.

The upper Keele succession is predominantly a clastic wedge, but dolomites within the unit continue to show positive $\delta^{13}C$ values. Thin limestone beds at the top of the formation record values as low as $-7‰$. Because the $\delta^{13}C$ of organic matter in these samples drops correspondingly, it is unlikely that the strong negative excursion is a secondary effect associated with subaerial exposure (cf. 28, 29). Isotopically light Keele limestones may genuinely predate Ice Brook glaciation,

but it is more likely that these are a basal facies of the "Tepee Dolomite," separated from underlying Keele rocks by a sequence boundary equivalent to the Ice Brook in other parts of the basin. This preferred alternative is consistent with known field relations and finds a parallel in coeval sections from South Australia, where siliciclastics and thin carbonates of the Seacliff Sandstone interfinger laterally with dolomites of the Nuccaleena Formation that cap Marinoan (= Varanger) glacial strata (30, 31).

Above the Ice Brook tillite, there is no further lithologic evidence for glaciation in the Windermere succession; however, within black shales and ribbon limestones of the Sheepbed Formation, there are two strong positive $\delta^{13}C$ excursions. In the carbonate profile, a peak of +6.7‰ occurs some 425 m above the base of the formation. Carbonates are absent in the succeeding 400 m of section but return near the top of the formation, where they record a second $\delta^{13}C$ excursion from values near 0‰ to +7‰ before falling to the moderate values that characterize overlying units. $\delta^{13}C$ values for organic carbon show a parallel trend but indicate that the lower excursion attains its maximum value within the middle, carbonate-free interval of the Sheepbed Formation. Stratigraphic relationships (32) preclude the interpretation of these excursions as a structural repeat of underlying units, but because carbonates are rare and siliciclastic lithologies are sparsely sampled, the full magnitude of the intervening negative excursion is unknown. Organic $\delta^{13}C$ values in the basal Gametrail Formation may suggest a further excursion, but they are not matched by equivalently light carbonates.

Comparable positive-to-negative $\delta^{13}C$ extremes bracket glaciogenic rocks, not only in the upper Windermere section but in every other tillite-bearing Neoproterozoic succession for which isotopic data are available (2). Thus, it is reasonable to hypothesize that the strong $\delta^{13}C$ variation in the middle Sheepbed corresponds to an interval of glaciation not documented by tillites in the Mackenzie Mountains. This predicts that, in correlative successions that contain two Varanger tillite intervals, both lower and upper tillites will be bracketed by strong C-isotopic excursions. Neoproterozoic successions in Spitsbergen provide a test of this hypothesis because they contain two discrete Varanger tillites separated by carbonate-bearing strata (33).

Chemostratigraphy of Tillite-Bearing Successions: Spitsbergen

The Neoproterozoic succession in northeastern Spitsbergen contains nearly 6 km of unmetamorphosed sedimentary rocks capped by an interval containing glaciogenic beds (34–36). From the base, thick siliciclastic sequences grade upward into carbonate-dominated facies deposited on a shallow marine platform. Bio- and chemostratigraphic correlations with radiometrically constrained strata elsewhere suggest that the Spitsbergen carbonate platform was established 750–800 Ma ago. Above the carbonates, glacial sediments occur in the Elbobreen and Wilsonbreen formations of the Polarisbreen Group (Fig. 2); these tillites are correlated throughout the North Atlantic region and are attributed to the Varanger Ice Age (37). The Elbobreen diamictite is thin and contains clasts derived almost entirely from underlying carbonates; some 250 m higher, the thick Wilsonbreen tillite is characterized by extrabasinal granitic, gneissic, and volcanic clasts (35). Both glacial intervals are capped by a thin unit of finely laminated dolomites succeeded by thicker dolomitic marls and shales.

Carbonates and organic matter in the thick subglacial platform display a C-isotopic profile closely similar to that determined for sub-Ice Brook units in the Mackenzie Mountains (Fig. 3). Units subjacent to the Polarisbreen Group correlate well with the Keele Formation—$\delta^{13}C$ in well preserved carbonates peaks at values as high as +11‰ and then declines to

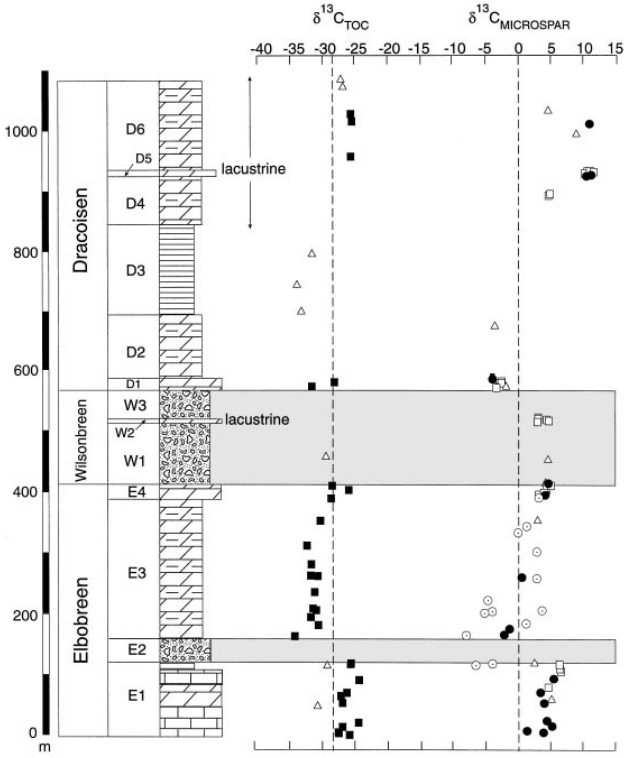

FIG. 2. Temporal variations in $\delta^{13}C$ of carbonates and coexisting organic matter in the Polarisbreen Group, Spitsbergen. The two Varanger glaciations are recorded in member E2 of the Elbobreen Formation and the Wilsonbreen Formation. The W2 dolomites are considered to represent glacio-lacustrine deposits (39). Similarly, carbonates in the D4-D6 interval of the overlying Dracoisen Formation likely formed in highly restricted to lacustrine environments (33, 35, 37). Analyses represented by open triangles are from Knoll *et al.* (4); squares represent analyses from Fairchild and Spiro (39). Open circles represent marly samples containing <50% carbonate; filled circles represent samples with >50% carbonate.

values as low as +2‰ just below the Elbobreen tillite; distinctive acritarchs in Spitsbergen and in Keele correlatives in northwestern Canada provide independent support for this correlation (38). Published C-isotopic profiles (4, 39) show a single negative excursion above the Wilsonbreen tillite; carbonates immediately below this tillite are relatively enriched in ^{13}C, much like those below the Elbobreen tillite. Until now, no C-isotopic data have been reported for the marly dolomites in the 150-m interval above the lower tillite. If the hypothesis generated from isotopic pattern in northwestern Canada is to survive, this previously unsampled interglacial interval in Spitsbergen must record strongly negative $\delta^{13}C$ values at its base followed by a rise to the high values seen in carbonates immediately beneath the Wilsonbreen tillite. As shown in Fig. 2, these rocks record strong $\delta^{13}C$ variations in both carbonates and organic C, with values in pure carbonates as low as −3‰ near the base of the interval and a sharp peak of +6‰ just below Wilsonbreen glaciogenic rocks.

Independent of other successions, the Spitsbergen record demonstrates that Varanger tillites record two discrete ice ages, each bracketed by strong secular variations in the global carbon cycle. The simplest chemostratigraphic correlation between Spitsbergen and northwestern Canada matches the successive troughs and peaks of the Tepee Dolomite and Sheepbed Formation with those of the Polarisbreen Group. A prediction of this correlation is that Sr-isotopic composition of Elbobreen Member E3 limestones will approximate values from Tepee limestones in the Mackenzie Mountains. A reported $^{87}Sr/^{86}Sr$ value of 0.7072 for a Tepee limestone sample (3) is close to the value of 0.7068 from

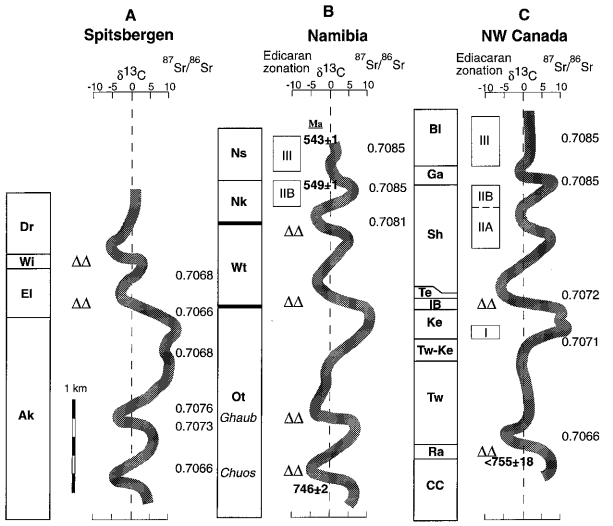

FIG. 3. Integrated chemo- and biostratigraphic correlation of terminal Proterozoic successions in (*A*) Spitsbergen, (*B*) Namibia, and (*C*) northwestern Canada. Note that data are plotted against stratigraphic thickness, which does not vary linearly with time; in particular, postglacial negative $\delta^{13}C$ excursions likely took place during relatively brief intervals of time. The bandwidth of $\delta^{13}C$ variations encompasses the majority of samples and is similar to $\delta^{13}C$ variations noted in shallow seawater today. The strong difference in Sr isotope compositions of well preserved limestones immediately above the lower and upper Varanger tillites suggests that the two glaciations can be distinguished even though $\delta^{13}C$ variations are similar. Fossil zonation scheme as explained in Fig. 1.; tillites are represented by double triangles; broad lines above and below the Witvlei Group in the Namibian column indicate stratigraphic breaks; radiometric ages are from Klein and Beukes (14), Hoffman *et al.* (41), and Grotzinger *et al.* (44). Stratigraphic abbreviations for northwest Canada as in Fig. 1; other abbreviations: Dr, Dracoisen Fm.; Wi, Wilsonbreen Fm.; El, Elbobreen Fm.; Ak, Akademikerbreen Group; Ns, Schwarzrand Subgroup of the Nama Group; Nk, Kuibis Subgroup of the Nama Group; Wt, Witvlei Group; Ot, Otavi Group.

a limestone in East Greenland that correlates with the E3 Member in Spitsbergen (4).

Thus, chemostratigraphic data from one of the best documented records of Varanger glaciation support the use of strong positive-to-negative $\delta^{13}C$ excursions as proxies for continental glaciation in Neoproterozoic successions. There are no glaciogenic beds lower in the Spitsbergen succession, but there are three distinct positive-to-negative $\delta^{13}C$ excursions, suggesting that earlier ice ages are recorded by glacial deposits elsewhere (ref. 4; two of the earlier biogeochemical events are shown in Fig. 3*A*). One of these likely correlates with the isotopic excursion above Rapitan glacials in the Mackenzie Mountains, and at least two may have equivalents in pre-Varanger tillites of Namibia.

Chemostratigraphy of Tillite-Bearing Successions: Namibia

In Namibia, glacial horizons traditionally have been used to correlate strata from two separate Neoproterozoic land masses. Between successions on the Congo and Kalahari cratons, however, there is considerable debate about stratigraphic relationships (5, 40). On the Congo Craton, thick pre-Varanger carbonates of the Otavi Group contain at least two tillite horizons separated by up to several hundred meters of limestone and dolomite. The Chuos Formation (Fig. 3*B*), which contains diamictites rich in basement clasts, iron-formation, and dropstones, is constrained by radiometric dates on underlying volcanic rocks to be younger than 746 ± 2 Ma (U-Pb zircon age; ref. 41). Recent sequence stratigraphic studies demonstrate that a second tillite (the Ghaub glacial interval) occurs some 400 m higher in the Otavi succession along the Fransfontein Ridge (42, 43); both Otavi tillites are bounded by ^{13}C-enriched carbonates below and ^{13}C-depleted carbonates above (43). Namibian successions thus provide both glaciogenic rocks and strong $\delta^{13}C$ variations to match with two of the three pre-Varanger $\delta^{13}C$ excursions in Spitsbergen. The Varianto diamictite, which occurs beneath tillites traditionally interpreted as Chuos equivalents in the Otavi Mountains, may provide the third; however, Hoffmann and Prave (42) recently have reinterpreted this unit as a direct Chuos equivalent, correlating overlying tillites in the Otavi Mountains with the newly discovered Ghaub glacial interval along the Fransfontein Ridge.

Glaciogenic rocks of likely Varanger age are preserved on the Kalahari Craton in two stratigraphically distinct horizons in the Witvlei Group and its equivalents in central Namibia. Based on chemo- and biostratigraphic relationships, we suggest in Fig. 3 that these rocks form the connection between older and younger strata on the Congo and Kalahari cratons. In the Witvlei area, only the lower of the two glacial deposits, the Blaubeker, is preserved; the upper tillite, the Blaskrans, occurs in thrust sheets of the Naukluft Nappe Complex and is correlated with an unconformity overlain by a cap carbonate within the Witvlei Group (40).

Carbonates of the uppermost Otavi Group are correlated here to immediately predate Witvlei strata; their strongly positive $\delta^{13}C$ values (*ca.* +10‰) match well with the Keele peak in the Mackenzie Mountains and with ^{13}C-enriched carbonates beneath Elbobreen tillites in Spitsbergen (4). In all three cases, $\delta^{13}C$ values drop from record high to moderate values before the first appearance of glaciogenic rocks. In the Nama Group, which lies conformably above the Witvlei, variations in $\delta^{13}C$ and Sr-isotopic abundances of limestones (3, 5, 44) are directly comparable to those in upper Windermere rocks of the Mackenzie Mountains. Both successions also contain Ediacaran fossils (Fig. 3). These bio- and chemostratigraphic correlations broadly constrain the two diamictites of the Witvlei Group to the Varanger Ice Age (11, 40). Above the lower Blaubeker, tillite reconnaissance sampling of carbonates from shallow to open marine facies shows negative $\delta^{13}C$ values (−2 to −4‰) near the base and ^{13}C enrichment upsection (up to +6‰ near the top). The lithostratigraphic correlation of the middle Witvlei unconformity with the Blaskrans tillite is supported by fine-scale sequence and chemostratigraphic trends above these surfaces in both areas. Both units begin with $\delta^{13}C$ values near −3‰ in finely laminated to massive dolomite facies and fall to near −5‰ in ribbon-laminated limestone facies at the maximum flooding surface (11). Preserved at this level are crystal fans of neomorphosed aragonite that have high Sr abundances (>1000 ppm) and $^{87}Sr/^{86}Sr$ values of 0.7081 (3). This $^{87}Sr/^{86}Sr$ value is significantly higher than those recorded in the Tepee Dolomite in the Mackenzie Mountains and the E3 equivalent in Spitsbergen, but it approximates values in carbonates just above the inferred biogeochemical proxy for late Varanger glaciation in northwestern Canada (Fig. 3). This suggests a Sr-isotopic distinction between the two ice ages and indicates a strong temporal change in seawater $^{87}Sr/^{86}Sr$ across the interval from the first Varanger glacial epoch to the second. This view supports the correlation of the Blaskrans tillite with Wilsonbreen diamictites and the positive-to-negative $\delta^{13}C$ excursion in the middle Sheepbed Formation, as well as the correlation of the Blaubeker, Elbobreen, and Ice Brook tillites (Fig. 3).

Discussion

Correlations with Australia. In Australia, where several glacial intervals have been identified in Neoproterozoic successions, reconnaissance C-isotopic data are consistent with the stratigraphic relationships described from Canada, Spits-

bergen, and Namibia. Negative $\delta^{13}C$ values are recorded in cap carbonates atop both Sturtian and Marinoan (= Varanger) tillites (45–47). Strongly positive $\delta^{13}C$ values (*ca.* +9.5‰), similar to the Keele peak, have been reported from carbonates beneath Marinoan glacial deposits in South Australia (48). Additional positive peaks (>+6‰) occur above the Marinoan interval in carbonates of the upper Wonoka Formation and upper Billy Springs Beds (48); an excursion to negative $\delta^{13}C$ values in intervening units of the lower Billy Springs Beds is associated with coarsely clastic rocks interpreted as glaciogenic (49). This sedimentological interpretation has been questioned (e.g., see ref. 48), but, in light of the hypothesis considered here, deserves further study. [Additional negative excursions in post-Marinoan carbonates of South Australia—in particular, remarkably negative (−8‰) $\delta^{13}C$ values in basinal limestones of the Wonoka Formation (48)—are not matched by equivalent ^{13}C depletion in cooccurring organic C (50); for this reason, we consider it unlikely that these carbonate values reflect the composition of contemporaneous surface seawater.] In central Australia, isotopic profiles based primarily on organic C data also show two post-Marinoan peaks separated by a negative excursion (50).

Recently, the lower of two Neoproterozoic tillites in northern Australia has been reinterpreted as an equivalent of Marinoan tillites in the southern and central parts of the continent (51, 52). This suggests that the upper tillite in this region may correlate with the Upper Varanger ice age in Spitsbergen and with the positive-to-negative C-isotopic excursions found in the Sheepbed Formation, Canada, and in post-Marinoan successions elsewhere in Australia.

The Discreteness of Neoproterozoic Ice Ages. The detailed correlations presented here indicate that Varanger glaciation occurred as two discrete ice ages, each associated with a strong positive-to-negative $\delta^{13}C$ excursion. A similar relationship between C-isotopic fluctuations and tillites in pre-Varanger sections from Namibia (42, 43) and northwestern Canada (7, 8, 15) suggests that the Neoproterozoic Earth experienced at least four (and perhaps five) separate glacial epochs. Ice ages may have been globally synchronous, but they were not everywhere equal in magnitude. As with the Cenozoic glaciations, major tillite accumulations in one region correlate with beds elsewhere that show little or no glacial influence. In such sections, only lowstand and/or biogeochemical data record glaciation. The confirmation that two C-isotopic oscillations characterize the Varanger interval indicates the potential for increased time resolution in terminal Proterozoic correlation, but as the two $\delta^{13}C$ peaks are comparable in magnitude, they may be difficult to distinguish in isolation. Sr-isotopic data, acritarchs, and Ediacaran fossils may aid in distinguishing between the first and second peaks.

The Genesis of Neoproterozoic Ice Ages. Secular variations in seawater $\delta^{13}C$ commonly are interpreted as the product of long term changes in the proportions of organic matter and carbonate buried in sediments (53, 54), but they may also reflect the episodic introduction of isotopically light carbon into the surficial ocean (5, 55, 56). The observation that all Neoproterozoic glacial epochs were preceded by intervals of pronounced ^{13}C enrichment in surface seawater suggests that high rates of organic carbon burial—perhaps associated with high sea level and continental break-up (57, 58)—facilitated glacial growth by reducing atmospheric greenhouse capacity. The downwarping of very high $\delta^{13}C$ values to more moderate values just below glacial deposits in some sections may indicate declining primary productivity associated with the establishment of surface refrigeration.

The inferred association of glacial onset with enhanced organic carbon burial is consistent with models that link Miocene climatic cooling to the formation of organic-rich sediments such as the Monterrey Formation, CA (59, 60). However, only the last of the four well documented Neoproterozoic ice ages is associated with a strong increase in seawater $^{87}Sr/^{86}Sr$. Thus, Neoproterozoic glaciation cannot be understood completely using Cenozoic models that link glacial expansion to the rise of the Tibetan Plateau and Himalayas (61).

The intimate association of deglaciation with cap carbonates characterized by low $\delta^{13}C$ values can be explained by the rapid turnover of poorly ventilated deep oceans (where organic matter was mineralized via sulfate reduction to CO_2 and HCO_3^-), possibly driven by glacial invigoration of deep circulation. This would have brought isotopically light dissolved inorganic carbon to the surface, with abundant CO_2 degassing into the atmosphere and melting the ice sheets, while the excess HCO_3^- in surface oceans drove the rapid precipitation of cap carbonates depleted in ^{13}C (55, 56). As noted by Kennedy (46), insofar as the precipitation of a mol of carbonate from bicarbonate in solution releases a mol of carbon dioxide, high rates of carbonate precipitation would further contribute to short term elevation of CO_2 levels (46). Massive release of methane from continental shelf and slope sediments provides a possible alternative for achieving simultaneous greenhouse warming, increased HCO_3^-, and ^{12}C enrichment in the surface ocean (62).

Because $\delta^{13}C$ minima coincide with maximum flooding surfaces of postglacial transgressions, it also has been proposed that postglacial $\delta^{13}C$ profiles may principally record the precipitation of ^{13}C-depleted carbonates in basinal waters most directly affected by upwelling, with increasing $\delta^{13}C$ values in overlying rocks reflecting progressive shallowing and, therefore, increasing lateral distance from isotopically light deep waters (46). Two observations militate against this interpretation. First, in Spitsbergen, negative C-isotopic excursions inferred to mark Sturtian glaciation occur in platform carbonates whose sedimentary features indicate deposition in coastal marine environments (4, 43). Second, postglacial $\delta^{13}C$ excursions are also well defined by organic C values; insofar as primary production occurred principally in the surface ocean, postglacial isotopic events must have affected surface and basinal water masses alike.

Plausible mechanisms of strong ^{13}C depletion, whether they involve oceanic overturn or mass mortality of primary producers, operate on relatively short time scales (63). Thus, the persistence of low C-isotopic values through considerable stratigraphic thicknesses above some tillites must reflect high rates of sediment accumulation (43, 46), especially carbonates precipitated from highly oversaturated surface waters.

The Timing and Pattern of Early Animal Evolution. In recent years, it has been common to view the end of the Varanger ice age and the diversification of Ediacaran animals as distinct events separated by millions of years. The correlations shown in Fig. 3 imply instead that Ediacaran animals originated before the Varanger Ice Age (Mackenzie assemblage I), began to diversify after the first Varanger glacial epoch (assemblage IIA), and radiated rapidly (assemblages IIB and III) after the second Varanger event. Post-Varanger Ediacaran assemblages are known from many localities worldwide; however, equivalents of assemblages I and IIB have not been identified outside of the Mackenzie Mountains, and we cannot rule out the possibility that their apparent low diversities reflect sampling and environmental factors as much as age. In particular, the diverse fronds of the Mistaken Point Formation, Newfoundland, cannot be placed confidently within the stratigraphic framework developed here, although their age of 565 ± 3 Ma (U-Pb age on zircons from interstratified ash beds; ref. 64) approximates recent age estimates for the close of the second Varanger ice age (11).

The oldest Ediacaran remains, thus, coincide in time with both the extreme ^{13}C enrichment documented in Keele and correlative strata and, at least approximately, independent evidence for increasing atmospheric oxygen levels based on

marked shifts in S isotopes recorded in marine sulfates and sulfides (65–67). During and after Varanger glaciation, the Sr- and C-isotopic records suggest further growth in atmospheric P_{O_2} (3, 68, 69), perhaps contributing to continuing Ediacaran diversification. Between these events, C-isotopes record rapid negative excursions whose only parallels in the Phanerozoic record mark mass extinctions (56); perhaps it is not coincidental that diverse and abundant fronds and trace fossils enter the geological record only after the second Varanger deglaciation. Just below the Proterozoic–Cambrian boundary, a final sharp $\delta^{13}C$ decline of more than 7‰ marks the stratigraphic breakpoint between faunas in which Ediacaran organisms were principal components and those dominated by Cambrian-style animals (70). Unlike earlier events, this negative excursion was not preceded by strong ^{13}C enrichment nor it is known to be associated with continental glaciation. Such correlations imply that the early evolution of macroscopic animals was closely tied to terminal Proterozoic environmental change, with some events—in particular the growth of atmospheric oxygen—speeding diversification, while others dampened it.

We thank P. F. Hoffman, N. P. James, J. M. Hayes, J. K. Bartley, and D. Des Marais for helpful comments and discussions. Research leading to this paper was supported in part by National Science Foundation Grant EAR 93-16238 (A.H.K., A.J.K.) and Natural Sciences and Engineering Research Council Grant A-2648 (G.M.N.).

1. Harland, W. B. (1964) *Geol. Rundschau* **54,** 45–61.
2. Kaufman, A. J. & Knoll, A. H. (1995) *Precambr. Res.* **73,** 27–49.
3. Kaufman, A. J., Jacobsen, S. B. & Knoll, A. H. (1993) *Earth Planet. Sci. Lett.* **120,** 409–430.
4. Knoll, A. H., Hayes, J. M., Kaufman, A. J., Swett, K. & Lambert, I. B. (1986) *Nature (London)* **321,** 832–838.
5. Kaufman, A. J., Hayes, J. M., Knoll, A. H. & Germs, G. J. B. (1991) *Precambr. Res.* **49,** 301–327.
6. Ross, G. M. (1991) *Geology* **19,** 1125–1128.
7. Eisbacher, G. H. (1981) *Geol. Soc. Can. Paper* **80,** 1–40.
8. Young, G. M (1992) *Geology* **20,** 215–218.
9. Aitken, J. D. (1991) *Geol. Soc. Can. Bull.* **404,** 1–43.
10. Aitken, J. D. (1991) *Geology* **19,** 445–448.
11. Saylor, B. Z., Kaufman, A. J., Grotzinger, J. P. & Urban, F. E. *J. Sediment. Res.* (in press).
12. Jefferson, C. W. & Parrish, R. R. (1991) *Can. J. Earth Sci.* **26,** 1784–1801.
13. Heaman, L. M., Lecheminant, A. N. & Rainbird, R. H. (1992) *Earth Planet. Sci. Lett.* **109,** 117–131.
14. Klein, C. & Beukes, N. J. (1993) *Econ. Geol.* **88,** 542–565.
15. Narbonne, G. M. & Aitken, J. D. (1995) *Precambr. Res.* **73,** 101–122.
16. Narbonne, G. M., Kaufman, A. J. & Knoll, A. H. (1994) *Geol. Soc. Am. Bull.* **106,** 1281–1292.
17. Hofmann, H. J., Narbonne, G. M. & Aitken, J. D. (1990) *Geology* **18,** 1199–1202.
18. Narbonne, G. M. (1994) *J. Paleo.* **68,** 411–416.
19. Popp, B. N., Takigiku, R., Hayes, J. M., Louda, J. W. & Baker, E. W. (1989) *Am. J. Sci.* **289,** 436–454.
20. Rau, G. H., Takahashi, T. & Des Marais, D. J. (1989) *Nature (London)* **341,** 516–518.
21. Freeman, K. H. & Hayes, J. M. (1992) *Global Biogeochem. Cycles* **6,** 185–198.
22. Strauss, H. & Moore, T. (1992) in *The Proterozoic Biosphere*, eds. Schopf, J. W. & Klein, C. (Cambridge Univ. Press, Cambridge), pp. 711–798.
23. Schidlowski, M., Eichmann, R. & Junge, C. E. (1975) *Precambr. Res.* **2,** 1–69.
24. Holland, H. D. & Beukes, N. J. (1990) *Am. J. Sci.* **290,** 1–34.
25. Des Marais, D. J., Strauss, H., Summons, R. E. & Hayes, J. M. (1992) *Nature (London)* **359,** 605–609.
26. Karhu, J. A. (1993) *Geol. Surv. Finland Bull.* **371,** 1–87.
27. Melezhik, V. A. & Fallick, A. E. (1996) *Terra Nova* **8,** 141–157.
28. Beeunas, M. A. & Knauth, L. P. (1985) *Geol. Soc. Am. Bull.* **96,** 737–745.
29. Rush, P. F. & Chafetz, H. S. (1990) *J. Sediment. Petrol.* **60,** 968–981.
30. Dyson, I. A. & von der Borch, C. C. (1994) in *Incised-Valley Systems: Origin and Sedimentary Sequences*, eds. Dalrymple, R. W., Boyd, R. & Zaitlin, B. A. (Society of Sedimentary Geology, Tulsa, OK), pp. 209–222.
31. Christie-Blick, N., Dyson, I. A. & von der Borch, C. C. (1995) *Precambr. Res.* **73,** 3–26.
32. Dalrymple, R. W. & Narbonne, G. M. (1996) *Can. J. Earth Sci.* **33,** 848–862.
33. Fairchild, I. J. & Hambrey, M. J. (1984) *Precambr. Res.* **26,** 111–167.
34. Knoll, A. H. & Swett, K. (1990) *Am. J. Sci.* **290,** 104–132.
35. Fairchild, I. J. & Hambrey, M. J. (1995) *Precambr. Res.* **73,** 217–233.
36. Hambrey, M. J. & Harland, W. B. (1985) *Palaeogeogr. Palaeoclimatol. Palaeoecol.* **51,** 255–272.
37. Fairchild, I. J., Hambrey, M. J., Jefferson, T. H. & Spiro, B. (1989) *Geol. Mag.* **126,** 469–490.
38. Kaufman, A. J., Knoll, A. H. & Awramik, S. M. (1992) *Geology* **20,** 181–185.
39. Fairchild, I. J. & Spiro, B. (1987) *Sedimentology* **34,** 973–989.
40. Hoffmann, K. H. (1990) *Commun. Geol. Surv. Namibia* **5,** 59–67.
41. Hoffman, P. F., Hawkins, D. P., Isachsen, C. E. & Bowring, S. A. (1996) *Commun. Geol. Surv. Namibia* **11**, 47–52.
42. Hoffmann, K. H. & Prave, A. R. (1996) *Commun. Geol. Surv. Namibia* **11,** 81–86.
43. Kaufman, A. J., Hoffman, P. F. & Bowring, S. A. (1996) *Geol. Soc. Am. Abstr. Prog.* **28**, A219.
44. Grotzinger, J. P., Bowring, S. A., Saylor, B. Z. & Kaufman, A. J. (1995) *Science* **270,** 598–604.
45. Williams, G. E. (1979) *J. Geol. Soc. (Australia)* **26,** 377–386.
46. Kennedy, M. (1996) *J. Sediment. Res.* **66,** 1049–1063.
47. Veizer, J. & Hoefs, J. (1976) *Geochim. Cosmochim. Acta* **40,** 1387–1395.
48. Jenkins, R. J. F. (1995) *Precambr. Res.* **73,** 51–70.
49. DiBona, P. A. (1991) *Q. Geol. Notes Geol. Surv. S. Australia* **117,** 2–9.
50. Walter, M. R., Veevers, J. J., Calver, C. R. & Grey, K. (1995) *Precambr. Res.* **73,** 173–196.
51. Plumb, K. A. (1996) *Geol. Soc. Australia Abstr.* **41,** 344.
52. Corkeron, M., Grey, K., Z. X. Li & Powell, C. (1996) *Geol. Soc. Australia Abstr.* **41,** 97.
53. Broecker, W. S. (1970) *J. Geophys. Res.* **75,** 3553–3557.
54. Hayes, J. M. (1983) in *Earth's Earliest Biosphere: Its Origin and Evolution*, ed. Schopf, J. W. (Princeton Univ. Press, Princeton), pp. 291–301.
55. Grotzinger, J. P. & Knoll, A. H. (1995) *Palaios* **10,** 578–596.
56. Knoll, A. H., Bambach, R. K., Canfield, D. E. & Grotzinger, J. P. (1996) *Science* **273,** 452–457.
57. Knoll, A. H. (1992) in *Origin and Early Evolution of the Metazoa*, eds. Lipps, J. H. & Signor, P. W. (Plenum, New York), pp. 53–84.
58. Des Marais, D. M. (1992) *Chem. Geol.* **114,** 303–314.
59. Vincent, E. & Berger, W. H. (1985) *Geophys. Monogr.* **32,** 455–468.
60. Raymo, M. E. (1994) *Paleoceanography* **9,** 399–404.
61. Raymo, M. E., Ruddiman, W. F. & Froelich, P. N. (1992) *Geology* **16,** 649–653.
62. Dickins, G. R., O'Neil, J. R., Rea, D. K. & Owen, R. M. (1995) *Paleoceanography* **10,** 965–971.
63. Kump, L. R. (1991) *Geology* **19,** 299–302.
64. Benus, A. P. (1988) in *Trace Fossils, Small Shelly Fossils, and the Precambrian-Cambrian Boundary*, eds. Landing, E., Narbonne, G. M. & Myrow (New York State Museum Bulletin, Albany, NY), Vol. 463, pp. 8–9.
65. Canfield, D. E. & Teske, A. (1996) *Nature (London)* **382,** 127–132.
66. Ross, G. M., Bloch, J. D. & Krouse, H. Roy (1995) *Precambr. Res.* **73,** 71–100.
67. Strauss, H. (1993) *Precambr. Res.* **63,** 225–246.
68. Derry, L. A., Kaufman, A. J. & Jacobsen, S. B. (1992) *Geochim. Cosmochim. Acta* **56,** 1317–1329.
69. Burns S. J. & Matter, A. (1993) *Ecolgae Geol. Helv.* **86,** 595–607.
70. Bartley, J. K., Pope, M., Knoll, A. H., Petrov, P. Yu., Semikhatov, M. A. & Sergeev, V. N. (1997) *Geol. Mag.* (in press).